Photochemical & Photobiological Sciences

Cite this: *Photochem. Photobiol. Sci.*, 2012, **11**, 1938

www.rsc.org/pps

PAPER

The interplay between hydrogen bonding and π–π stacking interactions in the crystal packing of N1-thyminyl derivatives, and implications for the photo-chemical [2π + 2π]-cycloaddition of thyminyl compounds†

Priscilla Johnston,[a] Ekaterina I. Izgorodina*[b] and Kei Saito*[a]

Received 29th June 2012, Accepted 16th August 2012
DOI: 10.1039/c2pp25228g

The solid-state photo-chemical dimerisation of thyminyl derivatives occurs when two thyminyl units are aligned in such a way that the olefinic moieties are separated by a distance of less than 4.2 Å. When irradiated with >270 nm UV, the thyminyl olefinic groups undergo [2π + 2π]-cycloaddition to form a dimeric cyclobutane derivative. However, the design and execution of [2π + 2π]-cycloaddition reactions can be challenging due to the requirement to produce molecular crystals with the necessary olefinic alignment. In this investigation, the crystallographic and solid-state photo-chemical reactions of six N1-thyminyl derivatives are studied. Only one derivative, thyminyl propanamide (**7**), was found to undergo [2π + 2π]-cycloaddition in the crystalline state. As such, quantum chemical methods were employed to study the photo-chemical transition states of the derivatives, as well as the strengths of typical intermolecular interactions that were observed in their crystal structures (such as π–π stacking between the thyminyl rings, Watson and Crick style hydrogen bonding and hydrogen bonding between functional groups of N1 substituents). These results were used to rationalise the solid-state photo-reactivity of more complex bis-thyminyl monomers.

Introduction

Topochemical reactions, such as the solid-state photo-chemical [2π + 2π]-cycloaddition, represent a common pathway to synthesise cyclic target molecules that possess precisely controlled stereochemistry. Such structural control over the photo-products has made possible the synthesis of complex or strained molecules, such as ladderanes,[1–3] cyclophanes,[2] hetero-dimers[4] and even some larger molecules, including oligomers and polymers.[4,5] Essentially, the [2π + 2π]-cycloaddition involves a photo-chemical reaction between two olefinic molecules (*via* combination of an excited-state and a ground-state species) to yield a cyclobutane derivative.[6] From a synthetic standpoint, the identification of high-yielding synthetic routes to cyclobutane compounds is worthy of pursuit, since cyclobutane moieties occur in a number of natural products and alkaloids.[7] However, the design and execution of [2π + 2π]-cycloaddition reactions can be challenging for a number of reasons.

Firstly, topochemical control of the reaction dictates that the pair of reacting olefins should be parallel to one another, and be separated by a distance of less than 4.2 Å.[8] Secondly, the stereoselectivity and photo-chemical yields of [2π + 2π]-cycloaddition reactions tend to be higher when the reactant molecules are irradiated as solids, rather than as solutions.[9] Therefore, to obtain the desired photo-products in useful quantities, one must effectively control the topochemistry of reactant molecules in the solid-state.

Molecular crystals of the reactants are certainly the ideal environments for reproducible stereoselective reactions, since molecules can pack in a rigid and regularly repeating manner. However, the rational-design of molecules for crystalline-phase [2π + 2π]-cycloaddition reactions remains challenging due to the difficulty in predicting the way a given compound will crystallise. Imparting control over the alignment of reactive groups can thus be an arduous process. Nevertheless, the field of crystal engineering has afforded a number of examples in which the reactant molecules have been designed to have a high probability of packing in the desired crystalline arrangement to favour the [2π + 2π]-cycloaddition. Exploited interactions have included non-covalent hydrogen bonding,[10] halogen-bonding,[11] and aromatic stacking;[4] metallic coordination atoms have also been used,[12–15] as well as molecular templates,[16–18] covalently linked spacers,[19] and inclusion compounds.[20–23]

[a]*Centre for Green Chemistry, Monash University, Wellington Road, Clayton, Australia, 3800. E-mail: kei.saito@monash.edu*
[b]*School of Chemistry, Monash University, Clayton, Victoria, Australia*

†Electronic supplementary information (ESI) available: Geometrical parameters of optimized transition-states; exemplary figures showing the optimised B3LYP structures of key interactions observed in the crystal structures; calculated numbers of interactions observed in the crystal structures; ^{1}H and ^{13}C NMR spectra of derivatives **4**, **6**, **7** and **9**; partial ^{1}H NMR spectra of irradiated **7** (solution-phase) and **9** (solid-phase). CCDC 888370, 888371, 888372, 888373 and 888374. For ESI and crystallographic data in CIF or other electronic format see DOI: 10.1039/c2pp25228g

In contrast to other molecules capable of [2π + 2π]-cycloaddition (*e.g.* derivatives of cinnamic acid,[24] coumarins,[25] stilbazoles,[26] *etc.*), comparatively fewer photo-active crystalline derivatives have been reported for thymine. Thymine, a nucleic acid in DNA, is well known to undergo dimerisation by [2π + 2π]-cycloaddition when exposed to UV radiation at wavelengths close to the thyminyl absorption maxima (>270 nm). The reverse reaction is also possible upon exposure of the photodimer to shorter UV wavelengths (220–250 nm).[27] In biological systems thymine photo-dimerisation has been implicated as a causative factor in certain types of cancer,[28,29] and much of the existing literature focuses on understanding thymine dimerisations in DNA systems.[30–32]

Since thymine is biologically derived and is also capable of the retro-[2π + 2π]-cycloaddition, we are interested in its potential use as a 'green' photo-reactive site in new monomer/polymer systems. Our research has concentrated on the design of bis-thyminyl monomers that can undergo reversible photo-polymerisation by a series of [2π + 2π]-cycloaddition reactions. These types of reversible polymers are important, because they expand the understanding of [2π + 2π]-cycloaddition and thymine photo-dimerisation in particular, but also this class of polymers could be used as recyclable plastics, self-healing polymers, or optical materials. Although we have already reported on the reversible topochemical photo-polymerisation of dimethyl 3,3′-(3,3′-(butane-1,4-diyl)bis(5-methyl-2,4-dioxo-3,4-dihydropyrimidine-3,1(2*H*)-diyl))dipropanoate crystals (Scheme 1),[33] understanding the structural factors necessary to achieve adequate monomer topochemistry is paramount to the design of new cyclobutane compounds and reversible polymers. In this paper we will present the results of a series of experimental and theoretical investigations that have enabled us to explain in more detail why certain monomer features lead to ideal topochemical arrangements for photo-polymerisation by the [2π + 2π]-cycloaddition.

We adopt a "bottom-up" approach to the understanding of photo-reactive bis-thyminyl monomers. Firstly, we investigate the solid-state photo-reactions of six simple N1 thyminyl derivatives: thyminyl acetic acid (**2**), thyminyl methyl acetate (**3**), thyminyl acetamide (**4**), thyminyl methyl propanoate (**5**), thyminyl propanoic acid (**6**) and thyminyl propanamide (**7**). Among the six monomers studied, only thyminyl propanamide **7** was successfully dimerised with UV radiation in the crystalline state. Secondly, the photo-reactivity of the monomers was studied through the concerted mechanism of the photo-induced [2π + 2π] cycloaddition using standard transition state theory[34] coupled with a correlated wavefunction-based method, MP2. Thirdly, quantum chemical calculations at the MP2 level of *ab initio* theory were also performed to study the strength of typical inter-molecular interactions observed in the crystal structures of N1 thyminyl derivatives, such as π–π stacking between the thyminyl rings, Watson and Crick style hydrogen bonding and hydrogen bonding between functional groups of N1 substituents. The outcomes of the quantum chemical study highlighted a series of structural and energetic factors affecting the topochemistry of the N1 thyminyl derivatives in the crystalline state and hence, their photo-reactivity towards photo-dimerisation. These computational results were then used to rationalise the solid-state photo-reactivity of bis-thyminyl monomers with the view of developing a strategy for a smart design of more complex bis-thyminyl monomers capable of photo-reactions in the crystalline state.

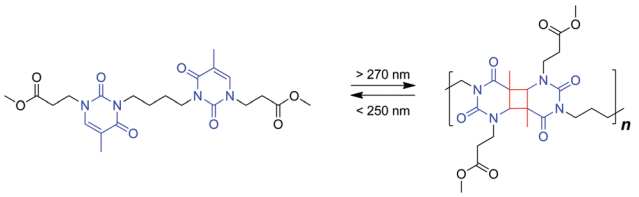

Scheme 1 Reversible photo-polymerisation of 3,3′-(3,3′-(butane-1,4-diyl)bis(5-methyl-2,4-dioxo-3,4-dihydropyrimidine-3,1(2*H*)-diyl))dipropanoate (**8**) by the [2π + 2π]-cycloaddition reaction of thyminyl units.[33]

Experimental

General

All chemicals were used as supplied by Sigma-Aldrich, and were of the highest available purity. ^{1}H- and ^{13}C-nuclear magnetic resonance experiments were conducted on a Bruker Avance 400 Spectrometer. All spectra were recorded at 25 °C, and referenced to the residual solvent signal. Infrared spectra were recorded using either a Perkin Elmer 2000 FT-IR spectrophotometer, in absorbance mode using KBr as the background reference; or, a Bruker Equinox 55 in ATR mode with diamond as the background reference.

X-ray diffraction

Due to the small or weakly diffracting crystals obtained for **3**, **5**, **6** and **9**, the reported structural analyses were performed on the MX1 micro-crystallography beam-line at the Australian Synchrotron, Clayton, Victoria. The end station comprised a φ goniostat with a Quantum 210r area detector. Data were collected using the Blue Ice GUI[35] and processed using the XDS software.[36] Due to hardware constraints (fixed detector angle, minimum detector distance) the maximum obtainable resolution at the detector edge was approximately 0.81 Å.

A single crystal of derivative **7** was coated in viscous oil and mounted on a glass fibre. Data ($2\theta_{max}$ 50–55°) were collected at 173(2) K using an Enraf Nonius KAPPA CCD and MoKα (λ 0.71073 Å) radiation. After integration and scaling, datasets were merged (R_{int} as quoted). Data were corrected for absorption using SORTAV.[37]

All the structures were solved and refined using the programs SHELXS-97[38] and SHELXL-97,[39] respectively. The program X-Seed[40] was used as an interface to the SHELX programs, and for preparation of the figures. Plausible positions of hydrogen atoms in water molecules, carboxylic groups and amides, were located in the difference Fourier map, and were refined such that O–H distances were restrained to reasonable values (0.88–0.98 Å); all other hydrogen atoms were placed in calculated positions using a standard riding model.

Synthesis of the N1-thyminyl derivatives (2–7)

2-(5-Methyl-2,4-dioxo-3,4-dihydropyrimidin-1(2*H*)-yl)acetic acid (2). Acetic acid, **2**, was synthesised according to a reported method.[41] A crystal structure has also been reported for this compound.[42]

Methyl 2-(5-methyl-2,4-dioxo-3,4-dihydropyrimidin-1(2*H*)-yl)-acetate (3). Methyl acetate **3** was prepared using a reported method.[43] Single crystals of **3** were obtained upon recrystallisation from hot EtOH.

Crystal data (CCDC 888370): $C_8H_{10}N_2O_4$, M = 198.18, colourless needle, 0.3 × 0.01 × 0.01 mm^3, monoclinic, space group $P2_1/n$ (no. 14), a = 5.0700(10), b = 22.070(4), c = 8.3100(17) Å, β = 100.85(3)°, V = 913.2(3) Å^3, Z = 4, D_c = 1.441 g cm^{-3}, F_{000} = 416, goniostat with quantum 210r detector, synchrotron radiation, λ = 0.71068 Å, T = 100(2) K, $2\theta_{max}$ = 50.0°, 5903 reflections collected, 1526 unique (R_{int} = 0.0522). Final *GooF* = 1.050, R_1 = 0.0469, wR_2 = 0.1204, R indices based on 1349 reflections with $I > 2\sigma(I)$ (refinement on F^2), 133 parameters, 0 restraints. Lp and absorption corrections applied, μ = 0.117 mm^{-1}. The measured completeness is low (0.956) due to the hardware limitations of the synchrotron beamline (*i.e.* fixed detector angle, minimum detector distance). However, the amount of observed data is close to 100% and yields a more than satisfactory refinement (R_1 = 0.0469). A short intermolecular contact was also observed between O7···C11 (2.96 Å), which was consistent with the Type I $O^{\delta-}\cdots{}^{\delta+}C{=}O$ (carbonyl–carbonyl) perpendicular interaction motif described by Allen *et al.*[44]

2-(5-Methyl-2,4-dioxo-3,4-dihydropyrimidin-1(2*H*)-yl)acetamide (4). Acetamide **4** was obtained by aminolysis of methyl acetate **2**. In this procedure, **2** (0.95 g, 4.8 mmol) was added to 15 equivalents of a concentrated aqueous ammonia solution. The flask was capped and the contents were shaken until the solid had completely dissolved. The title compound crystallised overnight from the resulting solution. A pure crystalline sample of **4** was obtained upon recrystallisation from H_2O. The NMR spectral data were consistent with literature data.

Yield: 0.72 g (82%). M.p. 297.5–300.2 °C (dec) (lit.[45] 299–302 °C, dec). MS (ESI$^-$): Calcd for $C_7H_9N_3O_3$: m/z 183.1; Found: m/z 182.2 (M − H). ^{1}H NMR (400 MHz, D_6-DMSO): δ_H 1.75 (d, J = 1.2 Hz, 3H, C5-CH$_3$), 4.23 (s, 2H, N1-CH$_2$), 7.18 (s, 1H, amide NH), 7.41 (d, J = 1.2 Hz, 1H, H6), 7.56 (s, 1H, amide NH). ^{13}C NMR (100 MHz, D_6-DMSO): δ_C 11.90 (C5-*C*H$_3$), 49.15 (N1-CH$_2$), 107.87 (C5), 142.42 (C6), 151.05 (C2), 164.50 (C4), 168.83 (CONH$_2$). Selected IR bands (KBr, cm^{-1}): 3410bs, 3296bs, 3156bs, 3076w, 3026bs, 2958w, 2934w, 2906w, 2860w, 2822w, 2774m, 1678bs, 1476s, 1418m, 1408m, 1396m, 1354m, 1230s, 1150m.

A crystal structure has already been reported for this compound.[46]

Methyl 3-(5-methyl-2,4-dioxo-3,4-dihydropyrimidin-1(2*H*)-yl)-propanoate (5). The title compound, **5**, was synthesised using a reported Michael addition reaction between methyl acrylate and thymine (**1**).[47] A crystalline sample was prepared upon recrystallisation of **5** from hot EtOH.

Crystal data (CCDC 888371): $C_9H_{12}N_2O_4$, M = 212.21, colourless plate, 0.40 × 0.10 × 0.02 mm^3, monoclinic, space group $P2_1/c$ (no. 14), a = 8.9270(18), b = 14.369(3), c = 7.7640(16) Å, β = 90.60(3)°, V = 995.8(4) Å^3, Z = 4, D_c = 1.415 g cm^{-3}, F_{000} = 448, goniostat with quantum 210r detector, synchrotron radiation, λ = 0.71253 Å, T = 100(2) K, $2\theta_{max}$ = 50.0°, 12566 reflections collected, 1702 unique (R_{int} = 0.2761). Final *GooF* = 1.059, R_1 = 0.0841, wR_2 = 0.2074, R indices based on 1572 reflections with $I > 2\sigma(I)$ (refinement on F^2), 143 parameters, 0 restraints. Lp and absorption corrections applied, μ = 0.113 mm^{-1}. As only weakly diffracting crystals were obtained for **5**, a large proportion of essentially "unobserved" reflections were used in the refinement which probably leads to the elevated value for R_{int} (0.276). Nevertheless, a satisfactory refinement was obtained (R_1 = 0.0841).

3-(5-Methyl-2,4-dioxo-3,4-dihydropyrimidin-1(2*H*)-yl)propanoic acid (6). The propanoic acid derivative **6**, was prepared by the base hydrolysis of the methyl ester **5**[47] (1.06 g, 5.0 mmol) in aqueous NaOH (1 M, 20 mL). The reaction mixture was heated at reflux for 3 h, and the solution was cooled and acidified to pH 2.0 with 10% HCl. The title compound, **6**, crystallised from the cooled solution (2 °C), and was washed repeatedly with H_2O. The NMR spectral data were consistent with literature data.

Yield: 0.90 g (91%). M.p. 181.7–182.9 °C (lit.[48] 172–174 °C). MS (ESI$^+$): Calcd for $C_8H_{10}N_2O_4$: m/z 198.1; Found: m/z 199.2 (M + H$^+$), 221.2 (M + Na$^+$). ^{1}H NMR (400 MHz, D_6-DMSO): δ_H 1.73 (d, J = 1.2 Hz, 3H, C5-CH$_3$), 2.59 (t, J = 7.2 Hz, 2H, CH$_2$CO), 3.81 (t, J = 7.2 Hz, 2H, N1-CH$_2$), 7.49 (d, J = 1.2 Hz, 1H, H6), 11.21 (s, 1H, NH). ^{13}C NMR (100 MHz, D_6-DMSO): δ_C 11.97 (C5-*C*H$_3$), 32.90 (*C*H$_2$CO), 43.94 (N1-CH$_2$), 108.17 (C5), 141.88 (C6), 150.80 (C2), 164.35 (C4), 172.33 (COOH). Selected IR bands (KBr, cm^{-1}): 3152s, 3090w, 3030s, 2978w, 2940w, 2812m, 1728s, 1696s, 1676s, 1474m, 1458m, 1436m, 1414m, 1402m, 1378m, 1356m, 1252m, 1226m, 1194m, 1160m, 1126m, 1054m.

Crystal data (CCDC 888372): $C_8H_{10}N_2O_4$, M = 198.18, colourless prism, 0.12 × 0.07 × 0.03 mm^3, monoclinic, space group $P2_1/n$ (no. 14), a = 4.9130(10), b = 20.405(4), c = 8.5920(17) Å, β = 101.90(3)°, V = 842.8(3) Å^3, Z = 4, D_c = 1.562 g cm^{-3}, F_{000} = 416, goniostat with quantum 210r detector, synchrotron radiation, λ = 0.71072 Å, T = 100(2) K, $2\theta_{max}$ = 50.0°, 8717 reflections collected, 1336 unique (R_{int} = 0.1273). Final *GooF* = 1.075, R_1 = 0.0577, wR_2 = 0.1552, R indices based on 1245 reflections with $I > 2\sigma(I)$ (refinement on F^2), 136 parameters, 0 restraints. Lp and absorption corrections applied, μ = 0.127 mm^{-1}. The measured completeness is low (0.903) due to the hardware limitations of the synchrotron beamline (*i.e.* fixed detector angle, minimum detector distance). However, the amount of observed data is close to 100% and yields a more than satisfactory refinement (R_1 = 0.0577). As only weakly diffracting crystals were obtained, a large proportion of essentially "unobserved" reflections were used in the refinement which probably lead to the elevated value for R_{int} (0.127).

3-(5-Methyl-2,4-dioxo-3,4-dihydropyrimidin-1(2*H*)-yl)propanamide (7). Thymine propanamide (**7**) was prepared by aminolysis of methyl propanoate **5**[47] (1 g, 4.7 mmol) using a similar procedure to that used for the synthesis of acetamide **4**. After recrystallisation from H_2O, pure **7** was isolated in 52% yield.

Yield: 0.48 g (52%). M.p. 233.9–235.8 °C. MS (ESI): Calcd for $C_8H_{11}N_3O_3$: *m/z* 197.1; Found: *m/z* 220.1 (M + Na). ^{1}H NMR (400 MHz, D_6-DMSO): δ_H 1.72 (d, J = 0.8 Hz, 3H, C5-CH_3), 2.42 (t, J = 6.8 Hz, 2H, CH_2–C═O), 3.80 (t, J = 6.8 Hz, 2H, N1-CH_2), 6.89 (s, 1H, amide NH), 7.40 (s, 1H, amide NH), 7.43 (d, J = 1.2 Hz, 1H, C6H), 11.19 (s, 1H, N3H). ^{13}C NMR (100 MHz, D_6-DMSO): δ_C 11.96 (C5-*C*H_3), 33.91 (*C*H_2CO), 44.39 (N1-CH_2), 107.92 (C5), 142.01 (C6), 150.75 (C2), 164.35 (C4), 171.69 (COOMe). IR (KBr, cm^{-1}): 3410m, 3364m, 3232m, 3188m, 3078m, 3048w, 2964w, 2932w, 2804w, 1686s, 1672s, 1658s, 1618s, 1472m, 1464m, 1448w, 1434w, 1386m, 1362m, 1242m, 1218m.

Crystal data (CCDC 888373): A crystal structure has been reported for this compound,[49] but the data presented below gave an improved refinement. $C_8H_{11}N_3O_3$, M = 197.20, colourless needle, 0.16 × 0.12 × 0.10 mm^3, monoclinic, space group $P2_1/c$ (no. 14), a = 7.3571(15), b = 15.243(3), c = 15.854(3) Å, β = 90.18(3)°, V = 1777.9(6) Å^3, Z = 8, D_c = 1.473 g cm^{-3}, F_{000} = 832, Nonius Kappa CCD, MoKα radiation, λ = 0.71073 Å, T = 173(2) K, $2\theta_{max}$ = 50.0°, 10 151 reflections collected, 2947 unique (R_{int} = 0.0408). Final *GooF* = 1.060, R_1 = 0.0370, wR_2 = 0.0814, R indices based on 2350 reflections with $I > 2\sigma(I)$ (refinement on F^2), 279 parameters, 0 restraints. Lp and absorption corrections applied, μ = 0.115 mm^{-1}. Although the measured completeness is 0.941, the amount of observed data is close to 100% and yields a more than satisfactory refinement (R_1 = 0.0370).

Synthesis of the N3-butyl bridged bis-thyminyl derivatives (8–10)

The syntheses and crystal structures of bis-methyl propanoate (**8**) and bis-propanamide (**10**) were described previously.[7]

3,3′-(3,3′-(Butane-1,4-diyl)bis(5-methyl-2,4-dioxo-3,4-dihydropyrimidine-3,1(2*H*)-diyl))dipropanoic acid (9). The bis-methyl propanoate monomer **8** (1.3 g, 2.8 mmol),[7] was heated to reflux in aqueous KOH (3 M, 30 mL) for 4 h or until the reaction mixture became a clear solution. Whilst still hot, the reaction mixture was rapidly acidified with 10% aqueous HCl to yield single crystals of the title compound. The crystals were filtered and washed repeatedly with H_2O.

Yield: 0.97 g, 80%. M.p. 236.8–239.2 °C. MS (ESI): Calcd for $C_{20}H_{26}N_4O_8$: *m/z* 450.18; Found: *m/z* 473.0 (M + Na, 100%). ^{1}H NMR: (400 MHz, D_6-DMSO) δ 1.47 (br, s (p), 4H, core CH_2), 1.78 (s, 3H, C5-CH_3), 2.61 (t, J = 6.8 Hz, 4H, *CH*$_2$CO), 3.78 (br, s (t), 4H, N3-CH_2), 3.87 (t, J = 6.8 Hz, 4H, 2 × N1-CH_2), 7.56 (s, 1H, C6H). ^{13}C NMR (100 MHz, $CDCl_3$): δ_C 12.54 (C5-CH_3), 24.60 (alk. CH_2), 32.70 (CH_2C═O), 40.10 (N3-CH_2), 44.95 (N1-CH_2), 107.27 (C5), 140.47 (C6), 150.64 (C2), 163.03 (C4), 172.22 (COOH). IR (ATR, cm^{-1}): 3498 m, 3071 m, 2930 m, 1714 m, 1691 m, 1621 s, 1434 m, 1383 m, 1357 m, 1205 m.

Crystal data (CCDC 888374): $C_{20}H_{30}N_4O_{10}$, M = 486.48, colourless prism, 0.07 × 0.03 × 0.01 mm^3, triclinic, space group $P\bar{1}$ (no. 2), a = 7.5950(15), b = 8.9000(18), c = 9.4540(19) Å, α = 96.93(3), β = 111.13(3), γ = 101.53(3)°, V = 570.9(2) Å^3, Z = 1, D_c = 1.415 g cm^{-3}, F_{000} = 258, goniostat with quantum 210r detector, synchrotron radiation, λ = 0.71069 Å, T = 100(2) K, $2\theta_{max}$ = 50.0°, 7070 reflections collected, 1854 unique (R_{int} = 0.0760). Final *GooF* = 1.083, R_1 = 0.0500, wR_2 = 0.1326, R indices based on 1685 reflections with $I > 2\sigma(I)$ (refinement on F^2), 167 parameters, 0 restraints. Lp and absorption corrections applied, μ = 0.114 mm^{-1}. The water molecule was refined such that O–H distances were restrained to reasonable values (0.88–0.98 Å). The measured completeness is low (0.924) due to the hardware limitations of the synchrotron beamline (*i.e.* fixed detector angle, minimum detector distance). However, the amount of observed data is close to 100% and yields a more than satisfactory refinement (R_1 = 0.0500).

Photo-reactivity studies

All of the [2 + 2]-cycloaddition reactions were performed using an Ultraviolet Products CL1000M UV-crosslinker lamp that produced mid-range UV-wavelengths centred at 302 nm.

Irradiation of solutions of 2–7. An aqueous solution of compound **7** (5 mL, 4.0–5.0 × 10^{-2} M) was transferred to a sealable pyrex tube (10 mL), purged with N_2, and then irradiated with 302 nm UV (0.35 kJ cm^{-2}). The solution was then freeze-dried and the resulting crude solids were subjected to ^{1}H NMR analysis in order to determine the extent of photo-dimerisation.

Irradiation of crystalline samples. Crystalline samples (approximately 100 mg) were irradiated as thin layers of crystals in uncovered petri dishes. The relevant irradiation doses are specified but generally ranged between 0–0.53 kJ cm^{-2}. All photo-reactions were monitored by ^{1}H NMR.

Theoretical procedures

Standard methods for the orbital approximation were used within GAUSSIAN 09.[50] All six thyminyl derivatives (thyminyl methyl propanoate, thyminyl propanoic acid, thyminyl methyl acetate, thyminyl acetic acid, thyminyl propanamide and thyminyl acetamide) were considered in the computational study. The geometry optimisations of the ground state of these thyminyl monomers and their dimers were performed at the B3LYP/6-31G(d) level of theory.[51–54] Improved electronic energies were obtained at the MP2 level of theory[55] in conjunction with the cc-pVTZ basis set.[56] The geometries of the monomers were conformationally screened to ensure the lowest energy structures. The dimers in this work were defined as two monomers non-covalently interacting through either π–π stacking or hydrogen bonding. The binding energies of dimers were calculated as the difference between the energy of the dimer and those of two monomers. All binding energies were corrected for zero-point vibration energy taken out of the B3LYP frequency calculations. Due to the similar size of the thyminyl derivatives studied the basis set superposition error (BSSE) was assumed to equally affect the binding energies of the dimers and therefore, time-consuming BSSE calculations were excluded from this study. Standard transition state theory[34] was used to locate transition states following the concerted mechanism of [2π + 2π] cycloaddition at the B3LYP/6-31G(d) level of theory for four thyminyl derivatives: methyl acetate **3**, propanoic acid **6**, methyl propanoate **5** and propanamide **7**. The monomers in their lowest energy

structures were taken for the transition state search. Four possible configurations of the transition state, such as *trans–syn* (TS), *trans–anti* (TA), *cis–syn* (CS) and *cis–anti* (CA) for each monomer were considered. Improved reaction barriers were calculated at the MP2/cc-pVTZ level of theory. The calculated reaction barriers were also corrected for zero-point vibration energy from B3LYP.

Results and discussion

To perform high yielding photo-chemical syntheses of thyminyl cyclobutane derivatives, the reactive olefins must be appropriately positioned in the crystal lattice, such that the olefinic groups align with one another and are separated by a distance of less than 4.2 Å.[8] In the literature to date, systematic studies concerning the photo-reactivity and crystal-packing behaviour of crystalline N1-thyminyl derivatives are limited to investigations involving 1-alkylthymines (from C_5H_{11} to $C_{10}H_{21}$)[57] and -alkylpropanoates (from C_9H_{19} to $C_{16}H_{33}$),[58] which possess long and weakly interacting alkyl chains. Thus, it was of interest to study the photo-reactivity and crystal packing behaviour of shorter-chain thyminyl derivatives, bearing either a CH_2CO or C_2H_4CO N1-spacer. In the previous studies, the thyminyl derivatives were decorated with only weakly interacting alkyl chains.[57,58] It is therefore important to examine how varying the N1 functionality between esters (**3** and **5**), carboxylic acids (**2** and **6**), and amides (**4** and **7**) can influence the molecular crystal packing through hydrogen bonding and π–π stacking interactions between the olefinic groups, and therefore the photo-reactivity of the crystalline derivatives.

Synthesis of the N1-thyminyl derivatives (2–7)

Thyminyl derivatives (**2–7**) were synthesised according to Scheme 2, in moderate to good yields. Briefly, thymine (**1**) was alkylated at the N1 position using bromoacetic acid to form the acetic acid derivative, **2**. The corresponding methyl ester **3** was obtained by H_2SO_4 catalysed esterification of acid **2** in methanol. Ester **3** was subjected to aminolysis using NH_3 to obtain amide **4**. Propanoate **5** was synthesised by Michael addition of methyl acrylate to thymine (**1**). The corresponding carboxylic acid (**6**) and amide (**7**) derivatives were subsequently formed by the base hydrolysis or aminolysis of ester **5**, respectively. The spectroscopic analyses of each derivative were consistent with previous literature reports or were in agreement with the proposed structures.

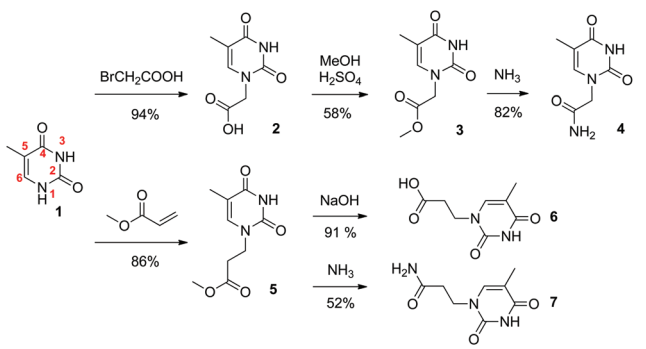

Scheme 2 The synthesis of the N1-thyminyl derivatives.

Solid-state dimerisation and the influence of crystal packing

Crystalline samples of the synthesised N1 derivatives were obtained from either ethanol (esters **3** and **5**) or water (acid and amide derivatives), and these samples were used for both the X-ray crystallographic and photo-chemical studies. The unit cells collected for crystals of **2** and **4** were consistent with previously reported crystal structures, and in these cases, references are made to the literature structures.[42,46] In order to examine the solid-state photo-reactivity of the thyminyl derivatives, the crystalline samples were each irradiated with 302 nm UV. However, only amide **7** was found to undergo [2π + 2π]-cycloaddition to form the corresponding cyclobutane dimer (Fig. 1).

Referring to Table 1, the crystal structures of compounds **2–6** each possessed olefinic separation distances of more than 4.2 Å, which accounted for their photo-stability. Only crystals of propanamide **7**, whose olefinic moieties were separated by 3.67 and 3.76 Å, underwent [2π + 2π]-cycloaddition to form the corresponding cyclobutane dimers in a total yield of 56%.

The crystal structure of **7** in Fig. 2 reveals a *trans–syn* (TS) type alignment between pairs of **7** prior to the irradiation. Therefore, according to the accepted topochemical arguments of Schmidt,[8] the main photo-dimer isomer should also possess the TS stereochemistry. Indeed, when the photo-dimerisation of **7** was followed throughout the irradiation (0–0.53 kJ cm^{-2}) using ^1H NMR, the TS isomer was the major cyclobutane dimer formed (obtained in 44% yield) (Figs. 1 and 2). Upon examination of the ^1H NMR spectrum of irradiated **7** (Fig. 1), some small amounts of the *cis–anti* (CA), *cis–syn* (CS) and *trans–anti* (TA) dimers were also detected; however, these species were

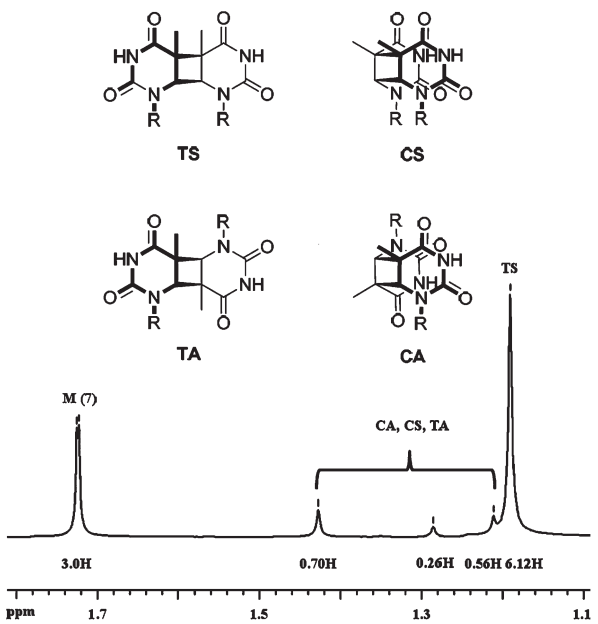

Fig. 1 Partial ^1H NMR spectrum of the irradiated sample of crystalline **7** showing peaks corresponding to the C5–CH_3 protons of monomer (M) and cyclobutane dimers (CA, CS, TA and the major product, TS).

Table 1 Measured distances (given in Å) of the observed interactions in the crystal structures of **2–7**

No.	Crystal system/ space group	Olefinic separation distance (Å)	Type of π–π stacking	WC HB (Å)	Inter-chain HB (Å)	Chain–ring HB (Å)
2	Monoclinic *P*21/*n* [42]	5.04	CS, slipped and displaced	2.05	NA	COOH···O═C4 1.88
3	Monoclinic *P*21/*n*	5.07	CS, slipped and displaced	1.95	NA	C2═O$^{\delta-}$···$^{\delta+}$C═O 2.96
4	Monoclinic *P*21/*c* [46]	5.21	TA, displaced sandwich	1.93[a]	$CONH_2$···O═CNH_2 2.14	$CONH_2$···O═C′2 2.14
5	Monoclinic *P*21/*c*	4.39	TA, sandwich	1.96	NA	NA
6	Monoclinic *P*21/*n*	4.91	CS, parallel displacement	1.97	NA	COOH···O═C′2 1.78
7	Monoclinic *P*21/*c*	3.67, 3.76	TS, criss-cross	NA	$CONH_2$···O═CNH_2 2.06, 1.90	$CONH_2$···O═C′2 2.02

[a] Anti-Watson and Crick hydrogen bonding was observed in the crystal structure of acetamide **4**.

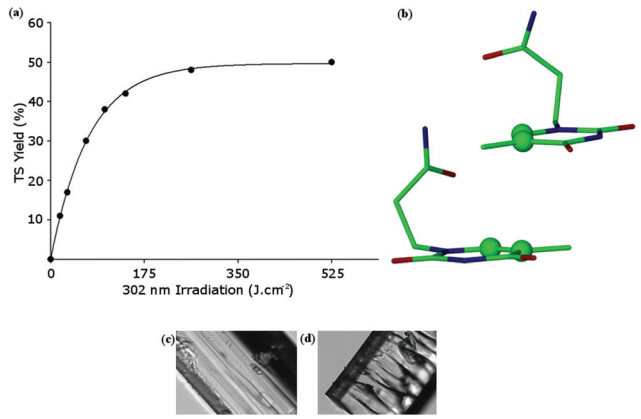

Fig. 2 (**a**) Follows the photo-dimerisation of **7** (crystalline-state) to the *trans–syn* (TS) cyclobutane derivative with 302 nm UV irradiation (0.53 kJ cm^{-2}). (**b**) The crystal structure of propanamide **7** (H atoms not shown) shows the TS alignment of the closest thyminyl pair. The carbons of the reactive olefinic groups are displayed as spheres. (**c**, **d**) The optical micrographs of the propanamide crystals before (**c**) and after (**d**) irradiation (magnification ×400) are also compared. The irradiated propanamide crystals (**d**) possess fracture lines.

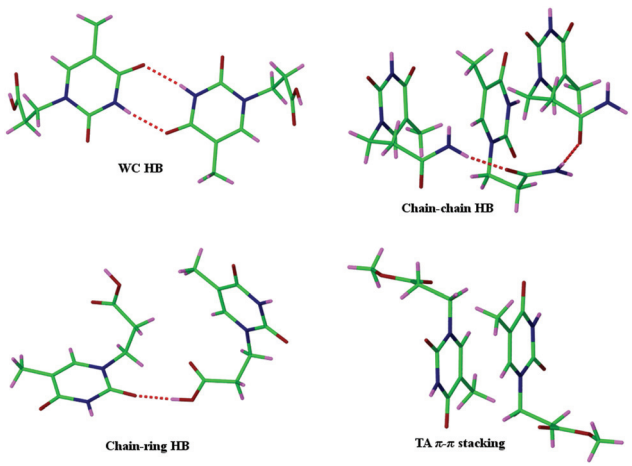

Fig. 3 Crystal structure examples of the: Watson and Crick hydrogen-bond (WC HB) in propanoic acid **6**; inter-chain HB in propanamide **7**; chain–ring HB in propanoic acid **6**; and TA π–π stacking in propanoate **5**.

only formed as minor photo-products. The formation of the other dimer isomers could result from either the destruction of the crystal lattice during photo-reaction or minor faults in the crystal packing of **7**. The accumulation of strain in the lattice as a result of small reorientations of the reacting molecules during photo-dimerisation is evidenced by the micrograph in Fig. 2d, which reveals severe fractures in the irradiated crystals of **7**.

To explain the photo-dimerisation success in the case of the propanamide derivative (**7**), a thorough analysis of the crystal structures of the six monomers was performed with the view of identifying the factors contributing to this result.

X-ray crystallography and structural comparison of the N1 derivatives

Examination of the crystal structures of **2–7** revealed several common features that are summarised in Table 1. Four typical intermolecular interactions were observed in the crystal structures of the six monomers: (1) π–π stacking interaction between the thyminyl rings, (2) Watson and Crick style hydrogen bonding (WC HB) between the thyminyl rings as shown in Fig. 3, (3) hydrogen bonding between terminal functional groups on the N1 substituents (Inter-Chain HB) and (4) hydrogen bonding between the carbonyl group on the thyminyl ring and functional group on the N1 substituent (chain–ring HB).

Analysis of Table 1 reveals that in most of the crystal structures, the monomers formed strong Watson and Crick style hydrogen bonds between the N3H···O═C4 and C4═O···HN3 groups of two adjacent thyminyl rings (Fig. 3). An anti-Watson and Crick hydrogen bond between N3H···O═C2 and C2═O···HN3 (Fig. 4c) was observed in the crystal structure of acetamide (**4**), while the propanamide did not form this type of intermolecular interaction. The lengths of the hydrogen bonds varied slightly between the N1 derivatives, but collectively ranged between 1.93 and 2.05 Å. Compared to the adenine–thymine base pair in DNA, which possesses hydrogen-

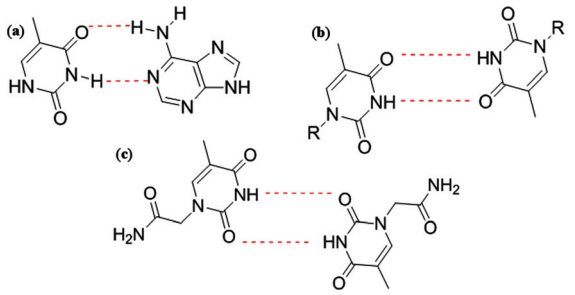

Fig. 4 (a) Watson and Crick hydrogen bonding between a thymine–adenine pair, (b) Watson and Crick style hydrogen bonding observed in the N1 thyminyl derivatives and (c) anti-Watson and Crick hydrogen bond observed between molecules of thyminyl acetamide **4**.

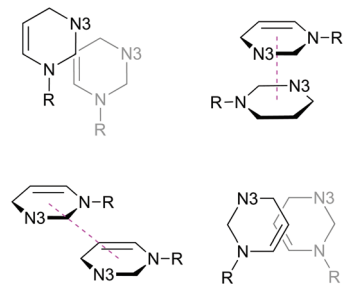

Fig. 5 Variations of the observed ring arrangements in crystals of **2–7**: (a) Slipped and displaced CS pair in **1** and **2**, (b) sandwiching in the TA pairs of **4** and **5**, and (c) parallel displacement in the CS pair in **6**, (d) criss-cross observed in the TS pair of **7**.

bond distances of 2.82 and 2.94 Å,[59] the Watson and Crick base pairing between thyminyl rings in the crystal structures of the N1 derivatives is much stronger. For N1 octyl thymine, the distance of the Watson and Crick hydrogen-bonds ranged between 2.77–2.88 Å.[60]

In the amide derivatives, **4** and **7**, inter-chain hydrogen bonding between an amide hydrogen atom and the amide carbonyl oxygen of a neighbouring molecule ($NH_2C{=}O\cdots HN(H)C{=}O$) appeared to be slightly stronger in the propanamide crystal as the measured hydrogen-bond distance of 1.94 Å was shorter than that of acetamide **4** (2.14 Å).[46] The longer bond distance in acetamide **4** may have been due to competition with the π–π stacking interactions between thyminyl rings, since in acetamide the TA-type sandwich arrangement (Fig. 5b) of the thyminyl rings was slightly displaced as a result of the inter-chain hydrogen bond.

In each of the N1 derivatives that possessed a hydrogen-bond donor atom (*i.e.* COOH and $CONH_2$) in the N1 chain, chain–ring hydrogen-bonding interactions were also observed. In amides **4** and **7**, the hydrogen bond occurred between an amide hydrogen atom and the C2 carbonyl oxygen of the thyminyl ring in a neighbouring molecule. Similarly in propanoic acid **6** the hydrogen bond occurred between the COOH hydrogen and the C2 carbonyl oxygen. However, in acid **2**, the chain–ring interaction occurred between the COOH hydrogen and neighbouring C4 carbonyl oxygen. The hydrogen bond to the C4 carbonyl oxygen in acid **4** was unusual considering that the C4 carbonyl oxygen was also involved in a partial Watson and Crick hydrogen bond to the N3 hydrogen of another thyminyl ring.

Another interesting chain–ring interaction was observed in the crystal structure of **3**. In this case, the C2 carbonyl oxygen and the ester carbonyl carbon of another molecule were closely associated (d = 2.61 Å). This $C{=}O^{\delta-}\cdots{}^{\delta+}C{=}O$ contact is a special type of interaction, which is based on weak electrostatic attractions between the polarised carbonyls, specifically the partially negative oxygen and partially positive carbon.[44]

From the crystal structures, it appeared that the Watson and Crick pairing stabilised the position of ring stacks, while the inter-chain and chain–ring interactions effected the arrangement of proximity related thyminyl ring pairs, thereby influencing the type of π–π interactions observed in the crystal structures. Co-operative effects between hydrogen-bonding environment and π–π stacking have also been proposed for base-stacking in DNA systems.[61] This idea is further strengthened when one considers the crystal structure of propanoate **5**, where the chain–chain and chain–ring interactions are absent, but Watson and Crick pairing is still observed. In methyl propanoate **5**, the proximity related thyminyl pairs are generated by TA sandwich stacking, whilst the position and separation between the stacked pairs is dictated by the length of the Watson and Crick hydrogen-bonds. Although propanoate **5** crystallises in the preferable TA thyminyl ring arrangement, the olefinic groups are separated by 4.4 Å, which is most likely too long for the [2π + 2π]-cycloaddition to occur.

CS displacements that were stabilised by chain–ring interactions were the most commonly observed packing arrangements (Fig. 5a,c). In methyl acetate **3**, the carbonyl–carbonyl ($C2{=}O^{\delta-}\cdots{}^{\delta+}C{=}O$) interaction led to the slipped and displaced CS packing. In propanoic acid **6**, $COOH\cdots O{=}C2$ and $C2{=}O\cdots HOOC$ hydrogen bonds produced displaced CS pairs; while a combination of chain–ring hydrogen bonding ($COOH\cdots O{=}C4$, $C4{=}O\cdots HOOC$) and WC hydrogen bonding contributed to the slipped and displaced CS ring packing in the crystal structure of acetic acid **2**. It is also interesting to note that the photo-reactive propanamide **7** crystals included a criss-cross orientation of the olefinic groups (Fig. 5d). This ring orientation was stabilised by extensive inter-chain and chain–ring hydrogen bonding, rather than a Watson and Crick hydrogen bond.

Of the six monomers only propanamide **7**, which displayed π–π stacking between the TS criss-crossed olefins, underwent photo-dimerisation. The remaining derivatives, **2–6**, were photostable. These observations prompted us to computationally investigate two aspects of the photo-chemical reactions. Firstly, it was of fundamental interest to determine whether the reaction barriers for the photo-induced [2π + 2π] cycloadditions vary when the N1 functionality is changed, or when different π–π stacking interactions (*i.e.* TA, TS, CA and CS) are adopted. Secondly, it was useful to examine the energetic differences between the four types of intermolecular interactions identified in the crystal structures described above, and to also investigate the roles that these interactions ultimately play in the topochemistry of the thyminyl derivatives in the crystalline state.

Substituent effects on reaction barriers for the concerted mechanism

To examine the reaction barriers, we studied the transition states for the concerted mechanism of the [2π + 2π] cycloaddition of thyminyl derivatives. It was shown recently that the photo-induced cycloaddition of thymine followed the concerted mechanism rather than the biradical pathway.[31] The latter was found to dominate during the thermal cycloaddition.[31] The photo-excitation of thymine results in a barrierless, non-radiative decay of a singlet excited state with a low-lying conical intersection between the ground state (S_0) and excited state (S_1) energetic profiles. At the S_0/S_1 conical intersection the system displays a fair degree of puckering around the C═C bond leading to a formation of the ground-state cyclobutane dimer. It was established that the concerted mechanism of cycloaddition could be accurately treated with a single-reference method, such as second-order perturbation theory, MP2.[62] For this reason the transition states for the concerted mechanism in the current study were located at the B3LYP/6-31G(d) level theory and the reaction barriers were then improved with MP2/cc-pVTZ. All of the transition states resembled the thymine dimer at the conical intersection in ref. 31 and displayed one imaginary frequency corresponding to the formation of the cyclobutane ring. Four possible configurations of the transition states, such as TA, TS, CA and CS, were calculated for four monomers: methyl acetate (**3**), propanoic acid (**6**), methyl propanoate (**5**) and propanamide (**7**) (see Fig. 6). The MP2 improved reaction barriers are presented in Table 2.

Reaction barriers for the same configuration vary only slightly by varying the N1 substituent. The TA and CA configurations produce the lowest reaction barriers. Energetically, the barriers vary from as low as 170 kJ mol^{-1} for the TA configuration in propanamide **7** to 323 kJ mol^{-1} for the CS configuration in propanoic acid **6**. Although the energetic difference in these barriers is quite significant, re-calculation to wavelengths shows that the barriers are well within the energy of 302 nm UV light.

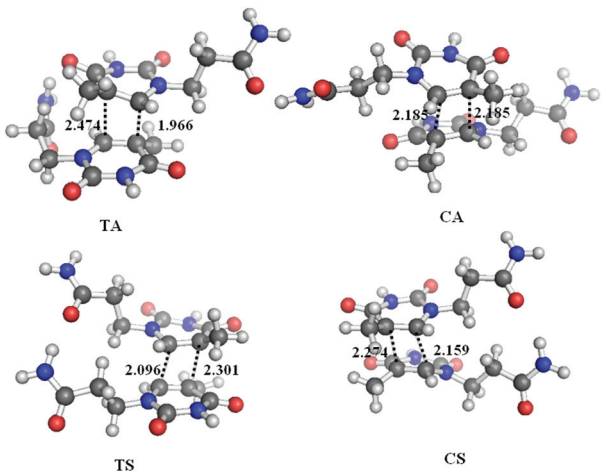

Fig. 6 Optimised structures of the transitions states for the concerted mechanism of photo-induced [2 + 2] cycloaddition of propanamide in four possible configurations: TA, CA, TS and CS. All distances are given in Å.

Table 2 MP2 reaction barriers for the concerted mechanism of photo-induced [2 + 2] cycloaddition

Monomer	Type of cycloaddition	$\Delta H^{\#}$, kJ mol^{-1}	ω, nm
Acetate (**3**)	TA	207.7	574.2
	CA	204.9	582.0
	TS	258.6	461.2
	CS	285.0	418.5
Propanoate (**5**)	TA	211.9	562.8
	CA	214.4	556.3
	TS	282.0	422.9
	CS	318.7	374.2
Propanoic acid (**6**)	TA	216.5	550.9
	CA	225.7	528.3
	TS	300.9	396.4
	CS	323.5	368.7
Propanamide (**7**)	TA	170.7	698.6
	CA	205.1	581.6
	TS	273.3	436.4
	CS	290.5	410.6

Therefore, regardless of the transition state configuration, the ring closure to form cyclobutane dimer should occur for all four monomers. This conclusion was confirmed by the solution-phase photo-dimerisation of **7**, in which all four photo-dimers were obtained in low yield (<7.5% total yield) and with reduced stereospecificity (see ESI†). From the solution-phase irradiation, the TS dimer of **7** was obtained with 8% specificity, whereas it was obtained with 80% specificity from the solid-state irradiation.

Apart from the CA configuration the transition states depict the asynchronous mechanism of the ring closure, with one forming C–C bond being longer than the other. For more details see the ESI.† Structurally, it requires a significant change in the ring and a perfect alignment of the C═C bonds with about 2 Å separation for the ring closure to occur. The monomers should not only align with the C═C bonds but they should also move closer to allow for cycloaddition. As a result, in the crystal structure we rely on the specific arrangement of the thyminyl rings, such that when the thyminyl derivates become excited upon UV exposure, they can move into the position that is most preferable for the ring closure to occur. This puts a constraint on the packing arrangement and the crystal structure should allow for a fair amount of flexibility for the thyminyl rings to adopt the preferred position. Out of the six monomers studied, three were crystallised in the CS slipped and displaced configuration that would not be ideal for the ring closure reaction and would require a high degree of rearrangement for the thyminyl rings. It can be noted that if the thyminyl rings are involved in other intermolecular interactions rather than π–π stacking, the flexibility of the rings in the crystalline state is rather limited and photo-dimerisation becomes highly unlikely. Thus, it appears that the packing arrangement plays a very important role in determining the extent of photo-dimerisation. The only successfully dimerised monomer crystal, propanamide **7**, displayed the TS criss-cross configuration (Fig. 1, Fig. 3d). In this arrangement the thyminyl rings would only need to slightly reorient for [2π + 2π]-cycloaddition to proceed. To summarise, as reactant topochemistry is the determinant factor in the outcome of any [2π + 2π] cycloaddition in the crystalline state, it appears that intermolecular interactions between monomers play a significant

role in accommodating the favourable π–π stacking to allow for photo-dimerisation. Therefore, the effect of the substituents on the packing arrangements of the N1 derivatives needs to be thoroughly investigated.

Substituent effects on strength of intermolecular interactions observed in the crystal structures

Secondly, to examine the strength of the various intermolecular interactions observed in the crystal structures of **2**–**7**, the specific intermolecular interactions were extracted from the crystal data and re-optimised at the B3LYP level of theory. The improved MP2 binding energies of the four types of intermolecular interactions (as shown in Fig. 3) as well as special cases (as shown in Fig. 7) are presented in Table 3. The first column of Table 3 shows the strength of the π–π stacking interactions modelled with respect to the preferable TA arrangement of thyminyl rings found in the methyl propanoate crystal structure. The geometry optimisations confirmed this arrangement for all but acetamide that preferred to optimise to the WC style hydrogen bonding instead (see Fig. 7). Similarly, the original π–π stacking arrangement found in the crystal structures apart from **3** were taken as initial geometries and three of the monomers, **2**, **6** and **7**, optimised to other intermolecular interactions shown under special cases 1 (SC1) in Table 3. Special cases 2 (SC2) shown in the last column represent intermolecular interactions observed in the crystal structures that do not fit the description of the four traditional types of interactions as depicted in Fig. 3.

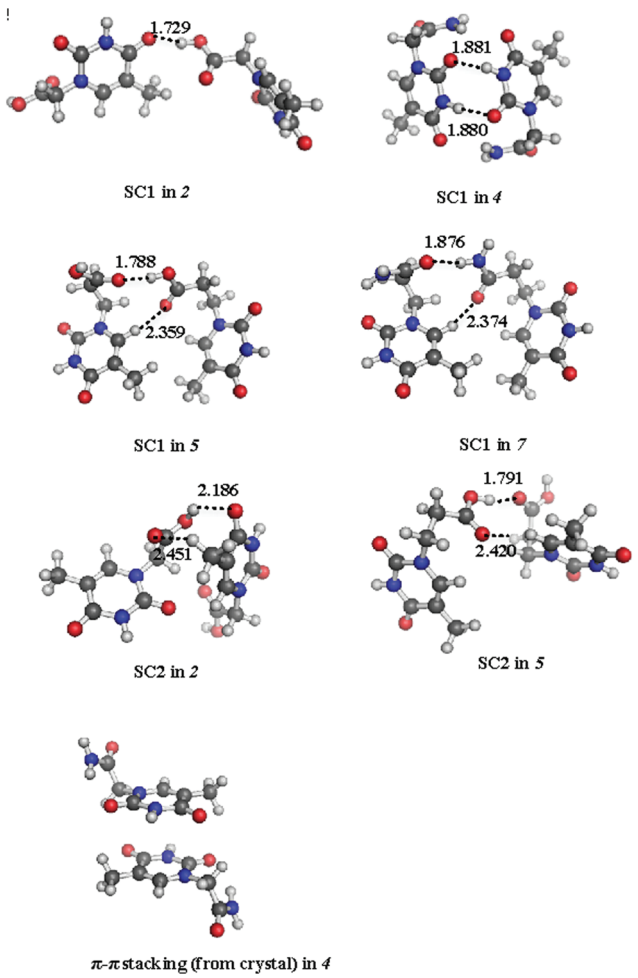

Fig. 7 Optimised structures of the special cases found in the crystal structures. All distances are given in Å.

Analysis of Table 3 reveals an interesting fact that for each monomer, regardless of the nature of the N1 derivative, the π–π stacking in the preferable TA arrangement and the classic WC hydrogen bonding differ only by a couple of kJ mol^{-1}, which is well within the systematic error of the calculations. The only exception is the dimer of acetic acid **2**, where the Watson and Crick hydrogen bonding is preferred by about 11 kJ mol^{-1} and might therefore prevent the thyminyl rings from stacking. Therefore, it is not surprising to find thyminyl rings in the crystal structure of acetic acid **2** in the CS slipped and displaced conformation that does not favour cycloaddition. Out of the six monomers, propanamide **7** produces the strongest π–π stacking and WC hydrogen bonding interactions in excess of >20 kJ mol^{-1}. In the case of acetamide **4**, the strength of the π–π stacking and WC HB interactions is similar to those of other monomers due to intramolecular hydrogen bonding between the carbonyl oxygen of the ring and the hydrogen atom of the amide group, preventing the formation of stronger inter-ring interactions. Due to the flexibility of the ethyl linker in propanamide **7** this intramolecular hydrogen bonding is absent in the monomer itself, thus resulting in a stronger WC hydrogen bond between the rings. It has to be noted that the thyminyl rings in the π–π stacking dimers (presented in the first and third columns of Table 3) are separated by about 3.7 Å on average regardless of the N1 derivative and the type of stacking. The calculations performed in gas phase usually produce shorter intermolecular distances (by about 0.5 Å)[63] than those observed in the crystal structure due to exclusion of interactions with the bulk of the crystal. This type of interaction decays very fast with distance ($\sim R^{-6}$) and at the separation of >5 Å could even become negligible.[64] For monomers with functionalities allowing for additional hydrogen bonding, such as carboxylic acids (**2** and **6**) and amides (**4** and **7**), inter-chain and chain–ring interactions are also relatively strong. The chain–ring interaction ranges from −48 kJ mol^{-1} for propanoic acid **6** to as much as −83 kJ mol^{-1} for propanamide **7**, making it the strongest interaction among the dimers studied. The inter-chain interaction in the dimer of acetic acid **2** is not only the strongest inter-chain interaction among the six monomers but also the strongest intermolecular interaction for acetic acid **2** overall.

The results on the MP2 binding energies indicate that for each individual monomer there is no significant variation in strength of the four main types of intermolecular interactions observed in the crystal structures. Therefore, all four types are in competition with each other and could potentially be present in approximately equal amounts in the crystals of the six monomers studied. In this study "ideal" interactions between two monomer units were considered. One should keep in mind that each monomer is usually involved in multiple intermolecular interactions at once, thus further strengthening some intermolecular interactions and weakening the others. The molecular arrangement in the crystal is thus a *subtle interplay* between not only

Table 3 Summary of the binding energies for intermolecular interactions observed in **2–7**

	π–π stacking TA[a]	WC HB	π–π stacking crystal	Inter-chain HB	Chain–ring HB	**SC1**[b]	**SC2**[c]
2	−43.5	−54.1	**SC1**	−69.4	−58.5	−47.5	−41.1
3	−54.0	−53.8	N/A	N/A	−47.0		
4	**SC1**	−59.7 −53.8[d]	−50.6	−53.7	−50.3	−76.1	
5	−53.9	−55.4	−53.9	N/A	N/A		
6	−49.6	−50.7	**SC1**	N/A	−48.3	−36.4	−38.5
7	−73.0	−75.6[d]	**SC1**	−55.6	−83.1	−71.3	

[a] Structures adapted to the TA configuration of the propanoate dimer observed in the crystal structure. [b] Optimized structures, for which the arrangement in the crystal produced a different configuration after geometry optimisation. These structures are denoted here as special cases 1 (SC1). [c] Special cases of the observed inter-molecular interactions between two thyminyl monomers that do not fit the description of the other four groups. These structures are denoted here as special cases 2 (SC2). [d] Anti-Watson and Crick HB as observed in the crystal structure.

the strength of individual intermolecular interactions, but also cooperativity effects of certain interactions, *e.g.* hydrogen bonding,[65] that in turn, might stabilise the crystal lattice to a much greater extent.

A thorough analysis of the crystal structures was performed, which concentrated on the number of specific intermolecular interactions per the same number of monomer molecules (ESI†). Acetic acid **2**, acetate **3** and propanoic acid **6** displayed an equal amount of WC and chain–ring hydrogen bonds per 8 monomer molecules, which was double the amount of the π–π stacking interactions. These observations are in agreement with the results obtained concerning the strength of these intermolecular interactions. In acetamide **4** anti-WC bonds, chain–chain and chain–ring interactions equally contributed to the packing arrangement of the monomer, whereas the π–π stacking constituted only 14% of the overall interactions. In these four cases the separation between the rings was too long, >4.9 Å, making the π–π stacking interaction too weak to drive the [2π + 2π] cycloaddition. In methyl propanoate **5**, the Watson and Crick HB dominated the crystal structure due to unavailability of the ester group to partake in other specific interactions. Although the π–π stacking in the preferable TA arrangement was still observed, the separation of 4.4 Å between the rings was quite long, potentially rendering this interaction relatively weak. In accordance with the computational results, a network of the chain–ring and inter-chain interactions was observed in propanamide **7**. The cooperativity of these specific interactions also allowed for a network of the TS criss-cross π–π packing to occur at a favourable separation of about 3.7 Å, thus making the latter a very strong interaction.

To this end, we can conclude that in order to encourage the formation of strong π–π stacking interactions between thyminyl rings in the preferable TA arrangement the energetic competition with specific chain–ring and inter-chain interactions should be eliminated. Three proposed strategies to achieve this goal were: blocking the N3 nitrogen of the thyminyl ring from forming the Watson and Crick style hydrogen bonding; including functional groups on the N1 derivatives that are less susceptible to hydrogen bonding (*i.e.* such as methyl propanoate); and finally, excluding the intramolecular interactions between the N1 chains and the ring by incorporating longer alkyl linkers, which will permit greater flexibility of the chains.

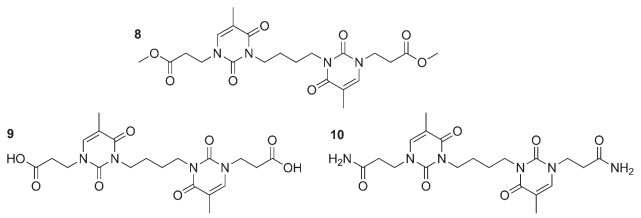

Fig. 8 N3–N3 butyl-linked derivatives.

Alkylation at the N3 position to eliminate Watson and Crick hydrogen bonding, and its influence on the crystal packing and photo-reactivity of the bis-thyminyl compounds

To address the strategies proposed in the computational section our research goal was to synthesise symmetrical bis-thyminyl derivatives (**8–10**, Fig. 8) by bridging two of the thyminyl units at the N3 position using an *n*-butyl spacer. This served two purposes. Firstly, N3–N3-alkyl bridging would effectively block the Watson and Crick hydrogen bonding, and; secondly, the additional thyminyl unit could potentially make the monomer system more rigid and hence, more susceptible to the preferred π–π stacking interactions.

The synthesis, crystallisation, and structure solutions of monomers **8** and **10** were described previously.[33] The bis-propanoic acid monomer, **9**, was obtained by base hydrolysis of the bis-methyl propanoate monomer, **8**. Single crystals of bis-propanoic **9**, suitable for photo-reactivity and X-ray analysis experiments were obtained by the rapid acidification of the hydrolysis reaction mixture.

Photo-irradiation study of bis-thyminyl derivatives, 8–10

To examine the photo-reactivity of the bis-thyminyl monomer crystals (**8–10**), samples of each compound were irradiated (0.30 kJ cm^{-2}), and the degrees of conversion to cyclobutane were determined by subsequent ^{1}H NMR analysis of the irradiated samples. The calculated ^{1}H NMR yields summarised in Table 4, were determined from the ratio of C5–CH_3 methyl protons of non-reacted thyminyl groups to the cyclobutane C5–CH_3 methyl protons. Referring to Table 4, it was evident that the bis-propanoate **8** and bis-propanoic **9** monomers underwent

Table 4 Interactions observed in the bis-thyminyl crystal structures when N3 is alkylated. All distances are given in Å

Cmpd.	System, space group	^{1}H NMR yield	Olefinic separation distance (Å)	Type of π–π stacking	WC HB	Inter-chain HB	Chain–ring HB
8	Monoclinic, $P21/c$ [33]	96	4.21 Å	TA, sandwich	NA	None	None
9	Triclinic, $P\bar{1}$	81	4.19 Å	TA, sandwich	NA	None	None
10	Tetragonal, $P42/n$ [33]	—	4.77 Å	CS, slipped and displaced	NA	CONHH···O═CNH2, 1.96 Å	CONHH···O═C2, 2.01 Å

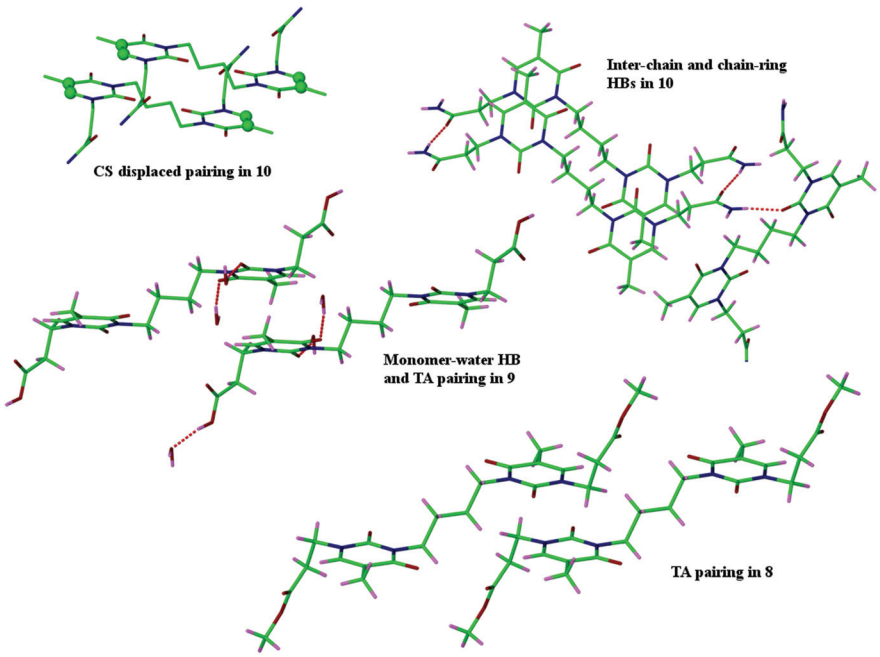

Fig. 9 Hydrogen bonding and π–π stacking interactions in the crystal structures of the N3-blocked bis-thyminyl monomers (**8–10**).

extensive photo-conversion to the corresponding cyclobutane compounds (96% and 81%, respectively). Conversely, the bis-propanamide monomer (**10**) was photo-stable. To understand the structural reasons contributing to the successful photo-conversion of monomer crystals of **8** and **9**, but not **10**, the crystal structures of each monomer were examined.

As mentioned, the crystal structures of monomers **8** and **10** were discussed in a recent report.[33] However, the crystal structure of the new monomer, bis-propanoic acid **9**, will be briefly discussed here. For convenience, some of the key interactions observed in the crystal structures of monomers **8–10** are presented in Table 4.

Due to the weakly diffracting nature of crystals obtained for **9**, the structure was determined from a single-crystal diffraction experiment performed on the micro-crystallography beamline at the Australian Synchrotron.

It was expected that inter-chain hydrogen-bond driven assembly of monomers would occur in the butyl-linked bis(propanoic acid) (**9**) crystals due to the free carboxylic moieties. However, instead of the anticipated intermolecular hydrogen bonding between monomer molecules, the interactions instead occurred between solvent and monomer molecules. Water molecules present in the crystal lattice from crystallisation actually provided sufficient hydrogen bonding sites to entirely eliminate inter-monomer hydrogen-bonding, and subsequently permit similar *trans–anti* thyminyl ring-stacking, to that observed in the bis-propanoate monomer structure, **8**.

The overall structure of **9** was stabilised by three unique hydrogen bonds between the monomer molecules and lattice included water molecules (Fig. 9). Each of the propanoic acid groups bonded with the O of a water molecule (COOH···O(W), 1.70 Å), while the hydrogen atoms of the water molecule participate in hydrogen-bonds with the thyminyl carbonyl oxygen atoms (H(W)···O═C4, 1.81 Å; and H(W)···O═C2, 1.93 Å). The closest thyminyl pairing arose from TA stacked rings, whose olefinic groups were separated by 4.19 Å.

Referring to Table 4, expectedly the alkyl bridging between the N3 positions eliminated Watson and Crick hydrogen bonding interactions entirely. Of further interest is that this modification also eliminated inter-chain and chain–ring hydrogen bonding between the bis-propanoic acid molecules (**9**), due to hydrogen bonding between monomer molecules and lattice included water molecules. The photo-reactive monomer crystals of **8** and **9**, also exhibited similar TA sandwich stacking (Fig. 9) between the proximity-related thyminyl rings; and in both cases, this was accompanied by the desired short olefinic separation distances of

4.21 and 4.19 Å, respectively. Not surprisingly, in the bis-propanamide monomer crystals (**10**), inter-chain hydrogen-bonding (NH···O═C, 1.96 Å) and chain–ring hydrogen bonding (amide NH···O═C2, 2.01 Å) gave rise to proximity-related CS thyminyl stacks that were slipped and displaced (Fig. 9). The displacement observed between the thyminyl moieties of molecules of **10** resulted in large olefinic separation distances of 4.77 Å that were inappropriate for [2π + 2π]-cycloaddition reactions.

It was found from this analysis that photo-reactive bis-thyminyl monomer crystals were obtained when Watson and Crick, inter-chain and chain–ring interactions were eliminated (*i.e.* in the cases of monomer crystals **8** and **9**). In both cases, the absence of these intermolecular interactions facilitated the preferable TA arrangement of thyminyl rings and close olefinic separation distances of around 4.2 Å.

Conclusions

For the N1 derivatives studied (**2–7**), the calculated reaction barriers for the concerted mechanism of photo-induced [2π + 2π] cycloaddition indicated energetic preference for the *trans–anti* and *cis–anti* arrangements of thyminyl rings. Although the reaction barriers were quite high (>170 kJ mol^{-1}), irradiation using 302 nm UV light provided sufficient amount of energy for their photo-dimerisation to occur for all four types of arrangements (TA, CA, TS and CS). The solution-phase irradiation of **7** supported this notion since the photo-reactions yielded mixtures of the photo-dimers in relatively low yields <10%, and with reduced stereospecificity.

The transition state analyses indicate that for the [2π + 2π]-cycloaddition to occur an appropriate alignment of the C═C bonds should be achieved. Out of the six monomers studied irradiation of the crystalline sample of the propanamide **7** resulted in dimerisation and produced mostly the *trans–syn* cyclobutane dimer in *ca.* 44% yield. The crystal structure of this particular derivative showed suitable π–π stacking between the thyminyl rings. Although propanoate displayed the preferred TA arrangement for the π–π stacking, the separation between the rings was relatively long for the cycloaddition to take place.

The strengths of the four specific interactions, such as π–π stacking, Watson and Crick, inter-chain and chain–ring hydrogen bonding, were subjected to rigorous computational studies with the view of quantifying the strength of each individual interaction. Strikingly, only a slight variation in the strength of these interactions was found for each monomer, thus highlighting the fact that the packing arrangement in the crystal was due to the *interplay* between the strength of the interaction and cooperativity effects. As a result, three strategies were proposed to encourage the formation of preferable π–π stacking arrangement: (1) Blocking the N3 nitrogen of the thyminyl ring, and thereby eliminating WC HB; (2) Inclusion of functional groups on the N1 derivatives that are less susceptible to hydrogen bonding; and (3) Exclusion of intramolecular interactions between the N1 chains and the ring by incorporating longer alkyl linkers.

Elimination of unfavourable Watson and Crick hydrogen bonding in the crystal was successfully achieved in bis-thyminyl derivatives **8–10**, upon installation of an *n*-butyl-bridge between two thyminyl rings. The rigidity of the rings led to favourable TA π–π stacking in **8** and **9**, whereas in **10** the inter-chain interactions between amide groups dominated the crystal structure. The best reversible photo-polymerisation was obtained in **8**, whose crystal structure was driven by the preferable TA arrangement of thyminyl rings in the absence of other specific interactions. In the case of **9**, the carboxylic groups were blocked from forming inter-chain interactions due to the presence of water molecules acting as stabilising agents, thereby leading to some degree of oligomerisation. In order to obtain more numerous photo-reactive bis-thyminyl derivatives, our future investigations will focus on varying the N3-bridge within a constant bis-methyl propanoate architecture. In doing so, it should also be possible to gain insight into the influence of different bridging species on the crystal packing and photo-reactivity of the resulting compounds. More crystallographic and quantum chemical studies will also be required to assemble a library of thyminyl derivatives that are amenable to chemical bridging and that also exhibit favourable π–π stacking arrangements for [2π + 2π]-cycloaddition reactions.

Notes and references

1 A. Jayaraman, V. Balasubramaniam and S. Valiyaveettil, Self-assembly of pentaphenol adducts: Formation of 3D network and ladder-type supramolecular structures in the solid state, *Cryst. Growth Des.*, 2006, **6**, 636–642.
2 T. Friščić and L. R. MacGillivray, Cyclophanes and ladderanes: molecular targets for supramolecular chemists, *Supramol. Chem.*, 2005, **17**, 47–51.
3 X. Gao, T. Friščić and L. R. MacGillivray, Supramolecular construction of molecular ladders in the solid state, *Angew. Chem., Int. Ed.*, 2004, **43**, 232–236.
4 G. W. Coates, A. R. Dunn, L. M. Henling, J. W. Ziller, E. B. Lobkovsky and R. H. Grubbs, Phenyl-perfluorophenyl stacking interactions: topochemical [2 + 2] photodimerization and photopolymerization of olefinic compounds, *J. Am. Chem. Soc.*, 1998, **120**, 3641–3649.
5 M. Hasegawa, Four-center type photopolymerization in the solid state, *Int. Chem. Eng.*, 1971, **11**, 177–188.
6 P. Klán and J. Wirz, in *Photochemistry of Organic Compounds*, John Wiley and Sons Ltd, 2009, pp. 227–453.
7 A. Sergeiko, V. V. Poroikov, L. O. Hanu and V. M. Dembitsky, Cyclobutane-containing alkaloids: origin, synthesis, and biological activities, *Open Med. Chem. J.*, 2008, **2**, 26–37.
8 G. M. J. Schmidt, Photodimerizations in the solid state, *Pure Appl. Chem.*, 1971, **27**, 647–678.
9 G. J. Fisher and H. E. Johns, Ultraviolet photochemistry of thymine in aqueous solution, *Photochem. Photobiol.*, 1970, **11**, 429–444.
10 X. Mei, S. Liu and C. Wolf, Template-controlled face-to-face stacking of olefinic and aromatic carboxylic acids in the solid state, *Org. Lett.*, 2007, **9**, 2729–2732.
11 T. Caronna, R. Liantonio, T. A. Logothetis, P. Metrangolo, T. Pilati and G. Resnati, Halogen bonding and π···π stacking control reactivity in the solid state, *J. Am. Chem. Soc.*, 2004, **126**, 4500–4501.
12 Q. Chu, D. C. Swenson and L. R. MacGillivray, A single-crystal-to-single-crystal transformation mediated by argentophilic forces converts a finite metal complex into an infinite coordination network, *Angew. Chem., Int. Ed.*, 2005, **44**, 3569–3572.
13 L. T. Ni, M. Nagarathinam and J. J. Vittal, Topochemical photodimerization in the coordination polymer $[\{(CF_3CO_2)(\mu\text{-}O_2CCH_3)Zn\}_2(\mu\text{-bpe})_2]_n$ through single-crystal to single-crystal transformation, *Angew. Chem., Int. Ed.*, 2005, **44**, 2237–2241.
14 G. S. Papaefstathiou, C. Milios and L. R. MacGillivray, A 2D metal–organic framework with two different rhombus-shaped cavities: a rare example of a (4,4)-net with alternating metal and organic nodes, *Microporous Mesoporous Mater.*, 2004, **71**, 11–15.
15 M. Yoshizawa, Y. Takeyama, T. Kusukawa and M. Fujita, Cavity-directed, highly stereoselective [2 + 2] photodimerization of olefins within self-

assembled coordination cages, *Angew. Chem., Int. Ed.*, 2002, **41**, 1347–1349.
16 L. R. MacGillivray, Organic synthesis in the solid state *via* hydrogen-bond-driven self-assembly, *J. Org. Chem.*, 2008, **73**, 3311–3317.
17 L. R. MacGillivray, J. L. Reid and J. A. Ripmeester, Supramolecular control of reactivity in the solid state using linear molecular templates [4], *J. Am. Chem. Soc.*, 2000, **122**, 7817–7818.
18 L. R. MacGillivray, J. L. Reid, J. A. Ripmeester and G. S. Papaefstathiou, Toward a reactant library in template-directed solid-state organic synthesis: reactivity involving a monofunctional reactant based on a stilbazole, *Ind. Eng. Chem. Res.*, 2002, **41**, 4494–4497.
19 I. G. Ovchinnikov, O. V. Fedorova, P. A. Slepukhin and G. L. Rusinov, Photoinduced template synthesis of cyclobutane-containing crown ether, *Russ. Chem. Bull.*, 2008, **57**, 212–214.
20 W. Herrmann, M. Schneider and G. Wenz, Photochemical synthesis of polyrotaxanes from stilbene polymers and cyclodextrins, *Angew. Chem., Int. Ed. Engl.*, 1997, **36**, 2511–2514.
21 W. Herrmann, S. Wehrle and G. Wenz, Supramolecular control of the photochemistry of stilbenes by cyclodextrins, *Chem. Commun.*, 1997, 1709–1710.
22 M. Pattabiraman, A. Natarajan, L. S. Kaanumalle and V. Ramamurthy, Templating photodimerization of *trans*-cinnamic acids with cucurbit[8]-uril and γ-cyclodextrin, *Org. Lett.*, 2005, **7**, 529–532.
23 K. S. S. P. Rao, S. M. Hubig, J. N. Moorthy and J. K. Kochi, Stereoselective photodimerization of (*E*)-stilbenes in crystalline γ-cyclodextrin inclusion complexes, *J. Org. Chem.*, 1999, **64**, 8098–8104.
24 Y. B. Ito Borecka, G. Olovsson, J. Trotter and J. R. Scheffer, Control of the solid-state photodimerization of some derivatives and analogs of *trans*-cinnamic acid by ethylenediamine, *Tetrahedron Lett.*, 1995, **36**, 6087–6090.
25 J. N. Moorthy and K. Venkatesan, Unusual photobehaviour of crystalline 7-methoxy-4-methylcoumarin, *J. Mater. Chem.*, 1992, **2**, 675–676.
26 M. Pattabiraman, A. Natarajan, R. Kaliappan, J. T. Mague and V. Ramamurthy, Template directed photodimerization of *trans*-1,2-bis-(*n*-pyridyl)-ethylenes and stilbazoles in water, *Chem. Commun.*, 2005, 4542–4544.
27 Y. Inaki and H. Hiratsuka, Reversible photo-cross-linking of polyvinyl alcohol containing thymine, *J. Photopolym. Sci. Technol.*, 2000, **13**, 739–744.
28 T. Carell and R. Epple, Repair of UV light induced DNA lesions: a comparative study with model compounds, *Eur. J. Org. Chem.*, 1998, 1245–1258.
29 G. M. Blackburn and R. J. H. Davies, The structure of thymine photodimer, *J. Chem. Soc. C*, 1966, 2239–2244.
30 W. J. Schreier, T. E. Schrader, F. O. Koller, P. Gilch, C. E. Crespo-Hernández, V. N. Swaminathan, T. Carell, W. Zinth and B. Kohler, Thymine dimerization in DNA is an ultrafast photoreaction, *Science*, 2007, **315**, 625–629.
31 M. Boggio-Pasqua, G. Groenhof, L. V. Schäfer, H. Grubmüller and M. A. Robb, Ultrafast deactivation channel for thymine dimerization, *J. Am. Chem. Soc.*, 2007, **129**, 10996–10997.
32 L. Blancafort and A. Migani, Modeling thymine photodimerizations in DNA: mechanism and correlation diagrams, *J. Am. Chem. Soc.*, 2007, **129**, 14540–14541.
33 P. Johnston, C. Braybrook and K. Saito, Topochemical photoreversible polymerization of a bioinspired monomer and its recovery and repolymerization after photo-depolymerization, *Chem. Sci.*, 2012, **3**, 2301–2306.
34 D. G. Truhlar, B. C. Garrett and S. J. Klippenstein, Current status of transition-state theory, *J. Phys. Chem.*, 1996, **100**, 12771–12800.
35 T. M. McPhillips, S. E. McPhillips, H. J. Chiu, A. E. Cohen, A. M. Deacon, P. J. Ellis, E. Garman, A. Gonzalez, N. K. Sauter, R. P. Phizackerley, S. M. Soltis and P. Kuhn, Blu-Ice and the distributed control system: software for data acquisition and instrument control at macromolecular crystallography beamlines, *J. Synchrotron Radiat.*, 2002, **9**, 401–406.
36 W. J. Kabsch, *J. Appl. Crystallogr.*, 1993, **26**, 795.
37 R. Blessing, Outlier treatment in data merging, *J. Appl. Crystallogr.*, 1997, **30**, 421–426.
38 G. Sheldrick, Phase annealing in SHELX-90: direct methods for larger structures, *Acta Crystallogr., Sect. A: Found. Crystallogr.*, 1990, **46**, 467–473.
39 G. M. Sheldrick, *SHELXL-97*, University of Göttingen, Göttingen, 1997.
40 L. J. Barbour, *Xseed*, University of Missouri, Columbia, 1999.
41 L. Kosynkina, W. Wang and T. C. Liang, A convenient synthesis of chiral peptide nucleic acid (PNA) monomers, *TetrahedronLett.*, 1994, **35**, 5173–5176.
42 M. C. Liu, W. Feng and J. C. Ding, 1-(Carboxymethyl)thymine, *Acta Crystallogr., Sect. E: Struct. Rep. Online*, 2004, **60**, o1611–o1612.
43 F. Debaene, J. A. Da Silva, Z. Pianowski, F. J. Duran and N. Winssinger, Expanding the scope of PNA-encoded libraries: divergent synthesis of libraries targeting cysteine, serine and metallo-proteases as well as tyrosine phosphatases, *Tetrahedron*, 2007, **63**, 6577–6586.
44 F. H. Allen, C. A. Baalham, J. P. M. Lommerse and P. R. Raithby, Carbonyl–carbonyl interactions can be competitive with hydrogen bonds, *Acta Crystallogr., Sect. B: Struct. Sci.*, 1998, **54**, 320–329.
45 J. Spychała, A convenient synthesis of monocationic 1-[(cyclic amidino)-methyl]thymines, *Synth. Commun.*, 1997, **27**, 3431–3440.
46 T. Borowiak, G. Dutkiewicz and J. Spychała, Molecular packing in (5-methyl-2,4-dioxo-1,2,3,4-tetrahydropyrimidin-1-yl) acetamide, *Acta Crystallogr., Sect. C: Cryst. Struct. Commun.*, 2006, **62**, o344–o345.
47 N. Robert, C. Hoarau, S. Célanire, P. Ribéreau, A. Godard, G. Quéguiner and F. Marsais, Efficient and fast Heck vinylation of 2-bromo-6-methyl pyridines with methylacrylate. Application to the synthesis of 6-methyl cyclopenta[*b*]pyridinone, *Tetrahedron*, 2005, **61**, 4569–4576.
48 S. Boncel and K. Walczak, Novel acyclic amide-conjugated nucleosides and their analogues, *Nucleosides, Nucleotides Nucleic Acids*, 2009, **28**, 103–117.
49 K. Kizawa, A. Takenaka and Y. Sasada, Structure of 1-(2-carbamoyl-ethyl)thymine, *Acta Crystallogr., Sect. C: Cryst. Struct. Commun.*, 1988, **44**, 535–537.
50 M. J. Frisch, G. W. Trucks, H. B. Schlegel, G. E. Scuseria, M. A. Robb, J. R. Cheeseman, J. A. Montgomery Jr., T. Vreven, K. N. Kudin, J. C. Burant, J. M. Millam, S. S. Iyengar, J. Tomasi, V. Barone, B. Mennucci, M. Cossi, G. Scalmani, N. Rega, G. A. Petersson, H. Nakatsuji, M. Hada, M. Ehara, K. Toyota, R. Fukuda, J. Hasegawa, M. Ishida, T. Nakajima, Y. Honda, O. Kitao, H. Nakai, M. Klene, X. Li, J. E. Knox, H. P. Hratchian, J. B. Cross, V. Bakken, C. Adamo, J. Jaramillo, R. Gomperts, R. E. Stratmann, O. Yazyev, A. J. Austin, R. Cammi, C. Pomelli, J. W. Ochterski, P. Y. Ayala, K. Morokuma, G. A. Voth, P. Salvador, J. J. Dannenberg, V. G. Zakrzewski, S. Dapprich, A. D. Daniels, M. C. Strain, O. Farkas, D. K. Malick, A. D. Rabuck, K. Raghavachari, J. B. Foresman, J. V. Ortiz, Q. Cui, A. G. Baboul, S. Clifford, J. Cioslowski, B. B. Stefanov, A. L. G. Liu, P. Piskorz, I. Komaromi, R. L. Martin, D. J. K. Fox, T. M. A. Al-Laham, C. Y. Peng, A. Nanayakkara, M. Challacombe, P. M. W. Gill, B. Johnson, W. Chen, M. W. Wong, C. Gonzalez and J. A. Pople, *Gaussian*, Gaussian Inc., Wallingford CT, 2009.
51 A. D. Becke, Density-functional exchange-energy approximation with correct asymptotic behavior, *Phys. Rev. A: At., Mol., Opt. Phys.*, 1988, **38**, 3098–3100.
52 C. Lee, W. Yang and R. G. Parr, Development of the Colle–Salvetti correlation-energy formula into a functional of the electron density, *Phys. Rev. B*, 1988, **37**, 785–789.
53 A. D. Becke, Density-functional thermochemistry. III. The role of exact exchange, *J. Chem. Phys.*, 1993, **98**, 5648–5652.
54 P. C. Hariharan and J. A. Pople, The influence of polarization functions on molecular orbital hydrogenation energies, *Theor. Chim. Acta*, 1973, **28**, 213–222.
55 C. Møller and M. S. Plesset, Note on an approximation treatment for many-electron systems, *Phys. Rev.*, 1934, **46**, 618–622.
56 J. Thom and H. Dunning, Gaussian basis sets for use in correlated molecular calculations. I. The atoms boron through neon and hydrogen, *J. Chem. Phys.*, 1989, **90**, 1007–1023.
57 Y. Inaki, E. Mochizuki, N. Yasui, M. Miyata and Y. Kai, Crystal structure and photodimerization of 1-alkylthymine: effect of long alkyl chain on isomer ratio of photodimer, *J. Photopolym. Sci. Technol.*, 2000, **13**, 177–182.
58 E. Mochizuki, N. Yasui, Y. Kai, Y. Inaki, W. Yuhua, T. Saito, N. Tohnai and M. Miyata, Crystal structure of long alkyl 3-(thymin-1-yl)propionates: style of hydrogen bonding and dependence on the alkyl chain length, *Bull. Chem. Soc. Jpn.*, 2001, **74**, 193–200.
59 M. Monajjemi and B. Chahkandi, Theoretical investigation of hydrogen bonding in Watson–Crick, Hoogestein and their reversed and other models: comparison and analysis for configurations of adenine–thymine base pairs in 9 models, *THEOCHEM*, 2005, **714**, 43–60.

60 N. Tohnai, Y. Inaki, M. Miyata, N. Yasui, E. Mochizuki and Y. Kai, Photoreactive and inactive crystals of 1-alkylthymine derivatives, *Bull. Chem. Soc. Jpn.*, 1999, **72**, 851–858.
61 J. Šponer, J. Leszczynski and P. Hobza, Hydrogen bonding, stacking and cation binding of DNA bases, *THEOCHEM*, 2001, **573**, 43–53.
62 B. Szefczyk, T. Andruniow and W. A. Sokalski, Ab initio multireference study of Hetero-Diels–Alder reaction of buta-1,3-diene with alkyl glyoxylates, *J. Mol. Model.*, 2008, **14**, 727–733.
63 G. B. Deacon, C. M. Forsyth, P. C. Junk, E. I. Izgorodina, T. J. Ness, G. Meyer and I. Pantenburg, A supramolecular twist to the structures of bis(polyfluorophenyl)mercurials, *CrystEngComm*, 2011, **13**, 88–92.
64 A. J. Stone, *The Theory of Intermolecular Forces*, Clarendon Press, Oxford, 1997.
65 D. Hadži, *Theoretical treatment of hydrogen bonding*, John Wiley and Sons, 1997.